

Analysis of Binding Affinities for Celecoxib Analogues with COX-1 and COX-2 from Combined Docking and Monte Carlo Simulations and Insight into the COX-2/COX-1 Selectivity

Melissa L. Plount Price and William L. Jorgensen*

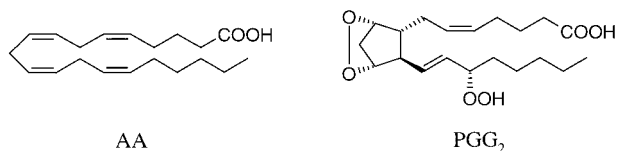
Contribution from the Department of Chemistry, Yale University, New Haven, Connecticut 06520-8107

Received March 22, 2000. Revised Manuscript Received July 21, 2000

Abstract: The origins of binding affinity and COX-2/COX-1 selectivity for analogues of celecoxib have been explored using an approach that combines docking with Monte Carlo (MC) simulations. These inhibitors are COX-2-selective nonsteroidal antiinflammatory drugs (NSAIDs) that are of current interest because the gastrointestinal irritation they cause is reduced compared to that caused by traditional NSAIDs. We report a novel docking method, based on a combined Tabu and Monte Carlo protocol, that determines starting conformations for MC simulations. Using the docking-predicted starting conformations, relative changes in binding free energies were computed for methyl, ethyl, hydroxymethyl, hydroxyl, thiomethyl, methoxy, trifluoromethyl, chloro, fluoro, and unsubstituted derivatives with the MC free energy perturbation (FEP) method. The computed free energies are in good accord with IC₅₀ values, and the structural information from the simulations can be used to explain the experimentally observed binding trends. In addition, the docking and FEP results have provided clarification of the binding conformation of the phenylsulfonamide moiety and the origin of COX-2/COX-1 selectivity. Namely, the COX-2 Val → COX-1 Ile substitution is accompanied by an unfavorable conformational shift of the phenylsulfonamide ring.

Introduction

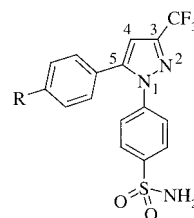
Nonsteroidal antiinflammatory drugs (NSAIDs) inhibit prostaglandin synthesis by blocking the cyclooxygenation of arachidonic acid (AA) to prostaglandin G₂ (PGG₂). PGG₂ is the precursor to numerous prostaglandins including those that possess analgesic, antipyretic, and antiinflammatory activity and those that provide protection for the gastric mucosa.



Until recently, a single cyclooxygenase (COX) enzyme was thought to be responsible for all of the catalysis of AA to PGG₂. It has now been shown that two isoforms of this enzyme, COX-1 and COX-2, exist.¹ COX-1 is expressed constitutively in most cells and is thought to be responsible for producing the prostaglandins that provide gastrointestinal tolerability. COX-2 is an inducible form that is present only in inflammatory states. Traditional NSAIDs such as aspirin, ibuprofen, and naproxen inhibit both isozymes, and this lack of selectivity explains the ulcerogenic side effects that chronic users of these drugs often experience.^{2–5}

- (1) Xie, W.; Chipman, J. G.; Robertson, D. L.; Erikson, R. L.; Simmons, D. L. *Proc. Natl. Acad. Sci. U.S.A.* **1991**, *88*, 2692–2696.
- (2) DeWitt, D. L. *Mol. Pharmacol.* **1999**, *4*, 625–631.
- (3) Marnett, L. J.; Kalgutkar, A. S. *Curr. Opin. Chem. Biol.* **1998**, *2*, 482–490.
- (4) Hawkey, C. J. *Lancet* **1999**, *353*, 307–314.
- (5) Vane, J. R.; Botting, R. M. *Clinical Significance and Potential of Selective COX-2 Inhibitors*; William Harvey Press: London, 1998.

Recently, a second generation of NSAIDs has been developed for the treatment of rheumatoid arthritis and osteoarthritis. These drugs selectively inhibit the COX-2 isozyme and differ clinically from traditional NSAIDs by having a reduced incidence of gastrointestinal irritation. One such drug, celecoxib **1**, marketed by Searle and Pfizer under the brand name Celebrex, shows a 375-fold selectivity of COX-2 over COX-1.⁶ No acute or chronic GI toxicity at dosage levels of this drug that showed severe toxicity in nonselective NSAIDs has been reported.^{7,8}



- 1** R = CH₃ Celecoxib (SC-58635)
2 R = Br (SC-558)

Celecoxib has also been shown to reduce UV light-induced tumor formation in mice⁹ and to have preventative activity

- (6) Penning, T. D.; Talley, J. J.; Bertenshaw, S. R.; Carter, J. S.; Collins, P. W.; Docter, S.; Graneto, M. J.; Lee, L. F.; Malecha, J. W.; Miyashiro, J. M.; Rogers, R. S.; Rogier, D. J.; Yu, S. S.; Anderson, G. D.; Burton, E. G.; Cogburn, J. N.; Gregory, S. A.; Koboldt, C. M.; Perkins, W. E.; Seibert, K.; Veenhuizen, A. W.; Zhang, Y. Y.; Isakson, P. C. *J. Med. Chem.* **1997**, *40*, 1347–1365.
- (7) Simon, L. S.; Weaver, A. L.; Graham, D. Y.; Kivitz, A. J.; Lipsky, P. E.; Hubbard, R. C.; Isakson, P. C.; Verberg, K. M.; Yu, S. S.; Zhao, W. W.; Geis, G. S. *J. Am. Med. Assoc.* **1999**, *282*, 1921–1928.
- (8) Simon, L. S.; Lanza, F. L.; Lipsky, P. E.; Hubbard, R. C.; Talwalker, S.; Schwartz, B. D.; Isakson, P. C.; Geis, G. S. *Arthritis Rheum.* **1998**, *41*, 1591–1602.
- (9) Pentland, A. P.; Schoggins, J. W.; Scott, G. A.; Khan, K. N. M.; Han, R. *Carcinogenesis* **1999**, *20*, 1939–1944.

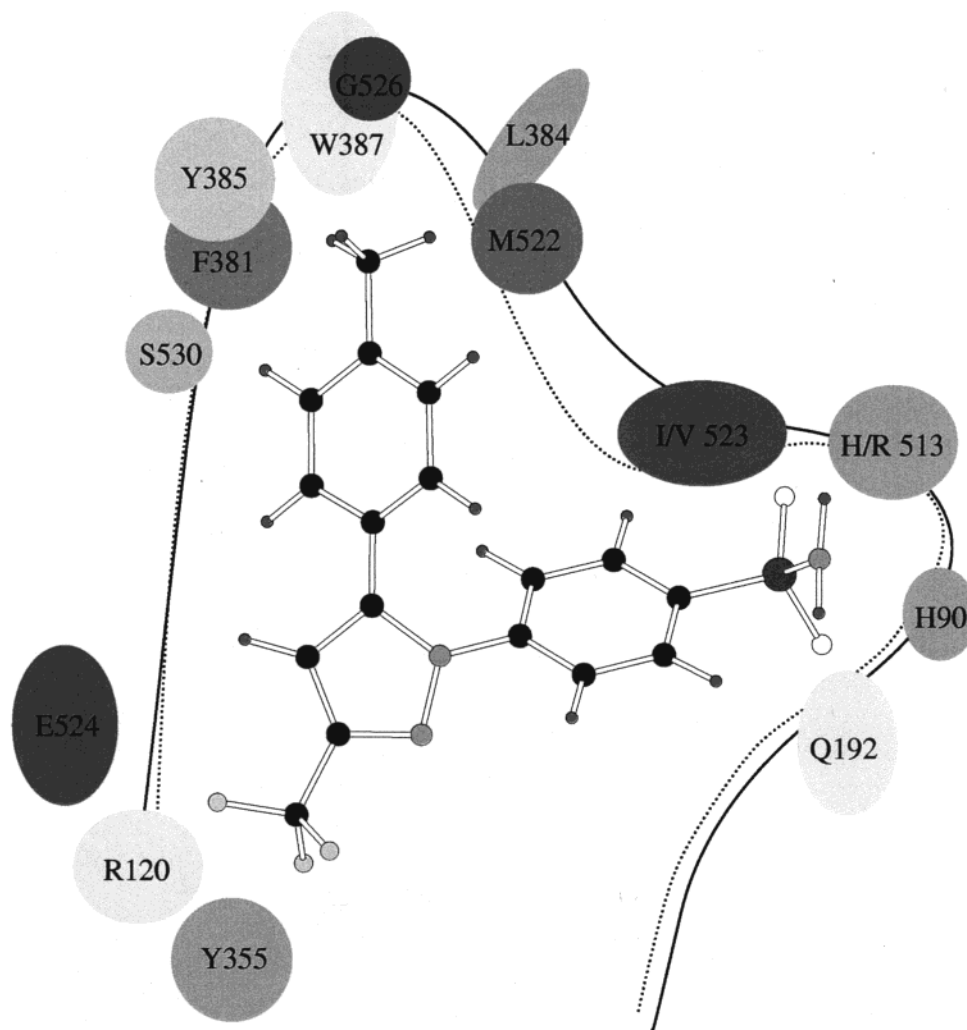


Figure 1. Schematic representation of the binding of celecoxib to COX-1 (dotted line) and COX-2 (solid line). The substitution of Ile 523 in COX-1 for Val in COX-2 is important in conferring COX-2 selectivity. All residue numbering refers to the COX-1 ovine sequence.¹³

against colon carcinogenesis.¹⁰ In fact, celecoxib has recently been approved by the FDA as the first drug for treatment of familial adenomatous polyposis, a hereditary disease that leads to colorectal cancer.¹¹ In addition, epidemiological studies suggest that COX-2-selective antiinflammatory drugs may become a new option in the treatment of Alzheimer's disease.¹²

The cyclooxygenase binding site in both isozymes is a long, narrow hydrophobic channel extending from the membrane-binding region of the protein. A schematic diagram, which is based on the crystal structures for COX-1¹³ and the complex of **2** with COX-2,¹⁴ is provided in Figure 1. At the entrance of the channel, Arg¹²⁰, Glu⁵²⁴, Tyr³⁵⁵, and His/Arg⁵¹³ form a network of hydrogen bonds that acts as a gate to the binding site. Llorens et al. recently proposed that the ability of different ligands to perturb this network determines the kinetics and contributes to the inhibitory selectivity.¹⁵

Unlike traditional NSAIDs that contain a carboxylate moiety that interacts with the salt bridge between Glu⁵²⁴ and Arg¹²⁰, the trifluoromethyl group in celecoxib does not provide this charge-charge interaction.¹⁴ While interactions with Arg¹²⁰ are not universally required for inhibition of COX-2 activity,¹⁶ mutagenesis studies have shown that ionic interactions of NSAIDs with this residue in COX-1 are critical for binding.¹⁷ Therefore, the presumably less favorable interaction of the trifluoromethyl group with the guanidinium group of Arg¹²⁰ may contribute to selectivity by destabilizing the ligand-COX-1 complex.

In the eastern side of the binding site (Figure 1), the sulfonamide group extends into a relatively polar side pocket that is somewhat restricted in COX-1. Based on site-directed mutagenesis experiments, the primary factor contributing to the COX-2 selectivity of celecoxib and related 1,5-diarylpyrazoles is the substitution of Ile⁵²³ in COX-1 for valine in COX-2.^{18,19}

(10) Kawamori, T.; Chinthalapally, V. R.; Seibert, K.; Bandaru, S. R. *Cancer Res.* **1998**, *58*, 409–412.

(11) Kovitz, C.; Hirsch, S. *Celebrex Receives FDA Approval As Adjunctive Treatment for Familial Adenomatous Polyposis (FAP)*, Searle healthNet, 1999. Available at <http://www.searlehealthnet.com/pr/pr122399.html>. Accessed February 7, 2000.

(12) Hull, M. F.; Feibich, B. L.; Schumann, K. L.; Bauer, J. *Drug Discov. Today* **1999**, *4*, 275–282.

(13) Picot, D.; Loll, P. J.; Garavito, R. M. *Nature* **1994**, *367*, 243–249.

(14) Kurumbail, R. G.; Stevens, A. M.; Gierse, J. K.; McDonald, J. J.; Stegeman, R. A.; Pak, J. Y.; Gildehaus, D.; Miyashiro, J. M.; Penning, T. D.; Seibert, K.; Isakson, P. C.; Stallings, W. C. *Nature* **1996**, *384*, 644–648.

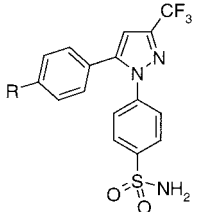
(15) Llorens, O.; Perez, J. J.; Palomer, A.; Mauleon, D. *Bioorg. Med. Chem. Lett.* **1999**, *9*, 2779–2784.

(16) Greig, G. M.; Francis, D. A.; Falgueyret, J. P.; Ouellet, M.; Percival, M. D.; Roy, P.; Bayly, C.; Mancini, J. A.; O'Neill, G. P. *Mol. Pharmacol.* **1997**, *52*, 829–838.

(17) Bhattacharyya, D. K.; Lecomte, M.; Rieke, C. J.; Garavito, M.; Smith, W. L. *J. Biol. Chem.* **1996**, *271*, 2179–2184.

(18) Gierse, J. K.; McDonald, J. J.; Hauser, S. D.; Rangwala, S. H.; Koboldt, C. M.; Seibert, K. *J. Biol. Chem.* **1996**, *271*, 15810–15814.

(19) Wong, E.; Bayly, C.; Waterman, H. L.; Riendeau, D.; Mancini, J. A. *J. Biol. Chem.* **1997**, *272*, 9280–9286.

Table 1. Experimental Activities for Celecoxib Analogues


compound	R	IC ₅₀ (μM) ^a	
		COX-1 ^b	COX-2
1	CH ₃	15.0	0.040
3	CH ₂ CH ₃	29.0	0.86
4	CH ₂ OH	> 1000	93.3
5	SCH ₃	—	0.009
6	OCH ₃	2.58	0.008
7	CF ₃	—	8.23
8	OH	—	> 100
9	Cl	—	0.01
10	F	—	0.041
11	H	—	0.032

^a Reference 6. ^b — = not used in this study.

However, the nearby His/Arg⁵¹³ replacement may also contribute to selectivity. Crystal structure data suggest that these residue differences improve access of the sulfonamide to a side pocket.^{14,20} However, there has been ambiguity concerning the orientation of the sulfonamide. Two X-ray structures of **2** bound to COX-2 (1cx2 and 6cox) solved from crystals formed in different space groups were reported simultaneously by the group at Searle.¹⁴ The position of the sulfonamide differs in these two structures, and the authors present a third conformation in their paper. This uncertainty is not surprising, considering that at the atomic resolution of these structures, hydrogen atoms cannot be visualized in the electron density maps, and the difference between oxygen and nitrogen atoms cannot be distinguished.

At the top of the hydrophobic channel is the region where catalysis occurs; here the 5-aryl ring of **2** makes hydrophobic contacts with Phe³⁸¹, Tyr³⁸⁵, Phe⁵¹³, Trp³⁸⁷, and Leu³⁸⁴. Comprehensive structure–activity relationship (SAR) studies have been performed at this site.⁶ In particular, monosubstitutions at the 4-position of this ring revealed several generalizations (Table 1). Hydrogen-bonding (**4** and **8**) and electron-withdrawing groups (**7**) yield diminished COX-1 and COX-2 affinity, while electron-donating groups (**5** and **6**) increase inhibition of both isozymes, although lower selectivity is observed. In addition, potency against COX-2 decreases with increasing steric bulk at this position (**3** and **7**).

Since no crystal structure is available for these 5-aryl derivatives other than **2** with COX-2 or for any of them with COX-1, we sought to (1) elucidate the structural features associated with these chemical modifications in order to explain the SAR data for COX-2 and (2) to clarify the origin of the COX-2/COX-1 selectivity. To this end, Monte Carlo simulations with free energy perturbation techniques (MC/FEP) were performed in order to obtain structures of the complexes and to calculate relative changes in free energies that occur upon binding. Previous studies have shown that this procedure produces structural and thermodynamic properties in good accord with experiment.^{21–23} Fortunately, computational resources have increased so that larger series of ligands can now be studied.

(20) Luong, C.; Miller, A.; Barnett, J.; Chow, J.; Ramesha, C.; Browner, M. F. *Nat. Struct. Biol.* **1996**, *3*, 927–933.

The usual procedure for assigning the initial structure of a protein–ligand complex in MC or molecular dynamics (MD) simulations has been to map it onto a closely related crystal structure. This protocol works when there are crystal structures for all of the receptor–ligand complexes or when the structural differences between the ligands are slight. However, in the present systems, several of the ligands (**3–6** and **8**) have an additional torsional degree of freedom compared to the ligand for which crystal structure data exist. The choice of this dihedral angle potentially influences the binding of the ligand. Clearly, to accurately calculate relative binding free energies, it is crucial that the appropriate conformation is sampled in the simulations. Due to the complexity of these systems and the presence of steric barriers, it is unclear that an incorrect starting geometry can be remedied in a reasonable amount of computer time. Therefore, to obtain the preferred binding conformations of these ligands, we have performed docking studies with our in-house program MATADOR (*metropolis and Tabu docking into organic receptors*).²⁴ The docking approach here involves predetermining likely binding conformations of the ligand, docking these low-energy conformers as rigid bodies, and then refining these structures. This multistep strategy is similar to the one reported by Wang, Kollman, and Kuntz,²⁵ although the method employed for each step differs. The structural results from the docking calculations were then used as initial positions for the MC/FEP simulations.

The present study is prototypical of a common drug design scenario in which limited structural data gives rise to uncertainties in ligand conformation and interpretation of SAR data. As shown here, combination of a docking protocol with a procedure for the accurate estimation of relative binding free energies can provide the desired clarification.

Computational Methods

System Preparation. Crystal structures (1prh¹³ and 1cx2¹⁴) from the Brookhaven Protein Data Bank provided Cartesian coordinates for murine COX-2 complexed with SC-558, **2**, and ovine COX-1 bound to flurbiprofen. The 1cx2 structure was chosen over the 6cox structure because the hydrogen atoms had already been assigned by the authors.¹⁴ The ethyl analogue **3** was modeled into both proteins on the basis of the crystal structure of **2** bound to COX-2, since the overall structures of the two isozymes are highly conserved. Protein residues with atoms greater than 15 Å from any atom of the ligand were removed for efficiency. The heme, bound at the peroxidase active site, was also removed since the majority of the molecule exceeded the cutoff radius. This trimming procedure reduced the number of explicit residues in the simulations to 148 for COX-2 and 149 for COX-1 including N-terminal methylacetamide and C-terminal acetate capping residues on noncontiguous pieces of the protein. Histidine residues 90, 95, 207, 386, and 388 were designated as δ-tautomers on the basis of visual inspection. Three lysine residues on the periphery of the system were neutralized to bring the total charge of the system to zero. The resulting systems were subjected to full conjugate gradient minimization using a distance-dependent dielectric constant of r . The OPLS-AA force field²⁶ provided all parameters except for the charges for the ligand atoms, which were obtained quantum mechanically as described below. The backbone of the energy-minimized protein was held rigid for all subsequent simulations involving SC-558 analogues **1** and **3–11**.

(21) Essex, J. W.; Severance, D. L.; Tirado-Rives, J.; Jorgensen, W. L. *J. Phys. Chem. B* **1997**, *101*, 9663–9669.

(22) Pierce, A. C.; Jorgensen, W. L. *Angew. Chem., Int. Ed. Engl.* **1997**, *36*, 1466–1469.

(23) Lamb, M. L.; Jorgensen, W. L. *J. Med. Chem.* **1998**, *41*, 3928–3939.

(24) Jorgensen, W. L.; van Hoorn, W. P.; Price, M. L. P. *MATADOR*, Version 1.0; Yale University: New Haven, CT, 1999.

(25) Wang, J.; Kollman, P. A.; Kuntz, I. D. *Proteins* **1999**, *36*, 1–19.

(26) Jorgensen, W. L.; Maxwell, D. S.; Tirado-Rives, J. *J. Am. Chem. Soc.* **1996**, *118*, 11225–11236.

Charges for inhibitors have often been derived by fitting to the electrostatic potential surface from ab initio 6-31G* calculations.²⁷ Recently, we reported a combined quantum mechanical (QM) and molecular mechanical method,²⁸ which uses charges from the CMIA procedure of Cramer and Truhlar.²⁹ The charges are derived via an empirical procedure that begins with an AM1 wave function and that has been parametrized to reproduce experimental gas-phase dipole moments. This method was tested in our laboratory through the computation of free energies of hydration. The current work also utilizes the CMIA charges, modified for use in an aqueous environment with the recommended scaling factor of 1.2,²⁸ for the ligands. They were determined for an initial low-energy conformer of each ligand and were kept constant throughout the MC simulations. The advantages of this method are three-fold. First, assignment of the charges is automatic; thus, the user need not assign OPLS-AA atom types. Second, the method eliminates the need to continually develop new atomic parameters for the force field, which is particularly cumbersome considering the complex combination of functionality typically found in druglike molecules. Finally, subtle charge differences between similar molecules are explicitly accounted for by the quantum mechanical calculations.

Conformer Selection for Docking. Most current docking programs incorporate some degree of flexibility into the system. However, explicitly including flexibility for just the ligand alone requires calculation of its intramolecular energy at each step in addition to consideration of many conformers that may not be conducive to binding. These issues can significantly add to the amount of computational time necessary to converge on the correct binding site orientation. An alternative is to predetermine which conformers are energetically favorable for the ligand and then to dock these conformers as rigid bodies.

A potential caveat in the search for relevant conformers is that the conformational preferences of the ligand in the gas phase or in solution may differ from the conformation of the ligand bound to a receptor. Thus, a range of low-energy conformers should be included. Furthermore, to reduce this bias for gas-phase preferences, a dielectric constant of 1.5 was used to scale the electrostatic interactions during the conformational searches,²⁵ which were performed with the BOSS program.³⁰ All conformers having an rmsd greater than 0.25 Å and energies within 3 kcal/mol of the global minimum were retained. For compounds **1**, **7**, and **9–11**, these criteria allowed us to select four unique conformers for use in the docking calculations. There were 8–25 conformers generated for compounds **3–6** and **8**, since these ligands have at least one extra torsional degree of freedom.

Docking Protocol. The system size was further reduced for the docking calculations by including only residues containing atoms within 6 Å from any ligand atom. To restrict the ligand to the binding site region, a restraining sphere was centered on C5 of the pyrazole in the crystal structure of **2** bound to COX-2. A half-harmonic potential of 20.0 kcal mol⁻¹ Å⁻² was applied if the distance from the ligand center to the sphere center exceeded 5 Å during docking.

A pseudo-Monte Carlo simulated annealing (MC/SA) approach was followed in which the Tabu algorithm was invoked in lieu of high-temperature runs. The Tabu algorithm was used as previously described.³¹ A recent comparison of four heuristic search algorithms indicated that the Tabu procedure was superior to the others for positioning a ligand as found in crystal structures during flexible docking.³² Test runs by us on several unrelated systems confirmed that the Tabu algorithm finds the crystal structure with greater frequency and at lower computational cost than a simulated annealing protocol.

(27) Carlson, H. A.; Nguyen, T. B.; Orozco, M.; Jorgensen, W. L. *J. Comput. Chem.* **1993**, *14*, 1240–1249.

(28) Kaminski, G. A.; Jorgensen, W. L. *J. Phys. Chem. B* **1998**, *102*, 1787–1796.

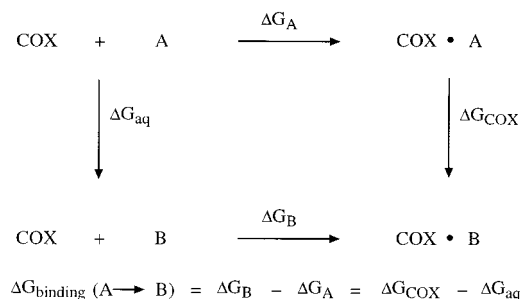
(29) Storer, J. W.; Giesen, D. J.; Cramer, C. J.; Truhlar, D. G. *J. Comput.-Aided Mol. Des.* **1995**, *9*, 87–110.

(30) Jorgensen, W. L. *BOSS*, Version 4.1; Yale University: New Haven, CT, 1999.

(31) Baxter, C. A.; Murray, C. W.; Clark, D. E.; Westhead, D. R.; Eldridge, M. D. *Proteins* **1998**, *33*, 367–382.

(32) Westhead, D. R.; Clark, D. E.; Murray, C. W. *J. Comput.-Aided Mol. Des.* **1997**, *11*, 209–228.

Scheme 1



It is possible that this improved efficiency is due to the facts that an optimal cooling schedule for the simulated annealing was not determined and that the success of the Tabu algorithm depends on fewer parameters.

Each ligand was subjected to five separate Tabu docking runs using MATADOR.²⁴ Each run included 120 cycles of Tabu searching, with each cycle generating 100 random structures and each Tabu list consisting of 25 configurations. The starting position of the ligand in each run was based on a random translation and rotation from the crystal structure position. Both the receptor and the ligand were treated as rigid bodies, although a new rigid conformer from the conformational search was exchanged for the current conformer every tenth time a new structure was generated. Docking results using this procedure are comparable to results from separate calculations on each conformer. The primary advantage of this method is that the user need only set up a single calculation.

Rigid-body energy minimization was performed in Cartesian space at each configuration in order to further improve the efficiency of finding the global minimum.³³ The interatomic nonbonded energies, calculated with the OPLS-AA force field and a distance-dependent dielectric of 4r, were stored on a spherical grid. Briefly, the spherical grid functions similarly to cubic grids,^{34–37} with the exception that the volume of the former is roughly half that of the latter. This feature reduces the memory required to store the grid points and the time spent initializing these points.

Using the complexes that were lowest in energy at the end of the Tabu docking, a series of four MC simulations was performed on each complex, where the temperature was lowered from 298 K to 3 K in three steps using 10⁵ configurations at each temperature. This procedure is similar to conventional simulated annealing in view of the temperature quenching. During the low-temperature MC simulations, the ligands were fully flexible but the protein remained rigid. As in the Tabu runs, the OPLS-AA force field, distance-dependent dielectric constant, and a spherical grid for nonbonded energy terms were used.

FEP Protocol. Changes in free energies were calculated with Zwanzig's equation³⁸ as previously described.^{21–23,39,40} The calculations yield the difference in binding free energies ($\Delta\Delta G_{\text{binding}}$) between molecules A and B according to Scheme 1, where the ligand A is mutated to B in solution and bound to the receptor. A single Z-matrix template containing the number of atoms present in the ethyl analogue **3** was used to build each subsequent ligand. For each new compound, the atomic number was changed or atoms were converted to dummy atoms as appropriate, and the CMIA charges were recomputed.

The lowest-energy structure from the docking calculations was used as the starting configuration in the bound MC/FEP simulations. This

(33) Trosset, J.-Y.; Scheraga, H. A. *J. Comput. Chem.* **1999**, *20*, 244–252.

(34) Goodsell, D. S.; Olson, A. J. *Proteins* **1990**, *8*, 195–202.

(35) Meng, E. C.; Shoichet, B. K.; Kuntz, I. D. *J. Comput. Chem.* **1992**, *13*, 505–524.

(36) Given, J. A.; Gilson, M. K. *Proteins* **1998**, *33*, 475–495.

(37) Goodford, P. J. *J. Med. Chem.* **1985**, *28*, 849–857.

(38) Zwanzig, R. W. *J. Chem. Phys.* **1954**, *22*, 1420–1426.

(39) Kollman, P. *Chem. Rev.* **1993**, *93*, 2395–2417.

(40) Jorgensen, W. L. *Computation of Free Energy Changes in Solution*. In *The Encyclopedia of Computational Chemistry*; Schleyer, P. v. R., Allinger, N. L., Clark, T., Gasteiger, J., Kollman, P. A., Schaefer, H. F., Eds.; John Wiley & Sons Ltd.: Chichester, 1998; pp 1061–1070.

same conformation may be used as the starting point for the simulations of the unbound ligand in solution as well, provided that the ligand is relatively rigid or that the conformational change that the ligand undergoes upon being transferred from solution to the receptor binding site is small. While the ligands in this study are relatively rigid, it was unclear whether different conformers for the ligands might exist in solution. Still's continuum GB/SA model^{41,42} as a treatment for solvation has yielded conformational results that are in agreement with more rigorous calculations for alanine dipeptide and 1,2-dichloroethane.⁴³ Therefore, a conformational search incorporating this solvation model was performed on each ligand; the lowest-energy structure was used as the starting point for the unbound MC simulations. The previously reported parameters for the surface area portion of the GB/SA term⁴² were modified for use with the OPLS-AA force field.

Each complex as well as each unbound ligand was hydrated by a sphere of 725 and 1483 TIP4P⁴⁴ water molecules, respectively, with a radius of 22 Å centered near the geometric center of the ligand. A half-harmonic potential with a 1.5 kcal mol⁻¹ Å⁻² force constant was applied to water molecules whose oxygen atom exceeded 22 Å from the center of the sphere, to prevent evaporation. A 9 Å residue-based cutoff was used for all nonbonded interactions. All internal degrees of freedom in the ligand were sampled in both the bound and unbound simulations. In the simulations of the complexes, the bond angles and dihedral angles of protein side chains in residues containing atoms within 10 Å of a ligand were sampled. The solvent was initially equilibrated for 5 million (M) configurations to remove any highly repulsive contacts with the solute(s). For each FEP window, an additional 10M and 20M configurations of equilibration were performed for the complex and unbound ligands, respectively.

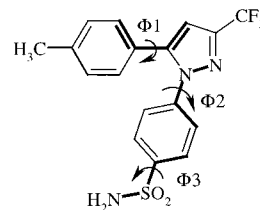
Following the equilibration period, free energy changes were averaged using windows with 5M configurations in the bound system and 10M configurations in the unbound case. Small perturbations (i.e., **5** → **6**, **9** → **10**, and **10** → **11**) were performed in five windows of double-wide sampling; all other perturbations were divided into 10 windows. Statistical uncertainties ($\pm 1\sigma$) for the free energy changes were computed with the batch means procedure using batch sizes of 250 000 configurations. All MC/FEP calculations were performed at 25 °C with the MCPRO program⁴⁵ using a PC cluster with ca. 50 Pentium processors.

Results and Discussion

Docking. Table 2 compares the structure of **2** from the 1cx2 entry to conformers of **1** generated during a conformational search and after the completion of the pseudo-MC/SA docking to COX-2. Note that all four unique conformers have relative energies within ca. 0.2 kcal/mol of each other, yet only two of the four conformers had the benzene rings positioned appropriately for binding. No conformer having the benzene rings rotated by 90° relative to each other (i.e., $\Phi_1 = \Phi_2 = 45^\circ$) was successfully docked.

The only conformation of the sulfonamide found during the docking positions a sulfonamide oxygen for interaction with Arg⁵¹³. This orientation disagrees with that of the 1cx2 crystal structure, where Arg⁵¹³ interacts with the sulfonamide nitrogen, but agrees with the orientation presented in 6cox. Docking of the rigid ligand conformer from the 1cx2 structure results in a complex lower in energy than the one predicted from docking of conformers generated from the conformational search. This is not surprising, considering that there is a bias since the

Table 2. Conformers of Celecoxib **1** Used in Docking Studies, Conformation of Docked Celecoxib, and Crystal Structure Conformer of **2**



conformer	Φ_1	Φ_2	Φ_3	relative energy (kcal/mol)
1a	45	45	90	0
1b	-45	-45	-90	0.08
1c	-45	-45	90	0.16
1d	45	45	-90	0.21
1c after docking	-45	-29	72	
2 crystal	-73	-16	-31	

complex was initially energy-minimized in the 1cx2 orientation. An optimal docking protocol would converge on the configuration of the complex that was "set" during the energy minimization as the global minimum, and thus there are some limitations to this procedure. As presented below, FEP results also indicate that the orientation in the 6cox structure is the correct alternative.

Analysis of the conformers in the rigid library explains why the sulfonamide was not predicted to bind in the 1cx2 orientation in these docking studies. As shown by the values for Φ_3 found in the conformational search (Table 2), the sulfonamide prefers to be perpendicular to the plane of the aryl ring ($\Phi_3 = \pm 90^\circ$) in the absence of the protein environment. In the binding site, the conformer having $\Phi_3 = -90^\circ$ places the two sulfonyl oxygen atoms in such a position that neither makes favorable electrostatic contact, whereas changing the dihedral by 180° ($\Phi_3 = 90^\circ$) allows each oxygen to make an O···H—N hydrogen bond (Figure 2). Presumably, the less favorable interactions with the protein formed by the former conformer reject it from docking as a rigid body. Once the rigid conformer with $\Phi_3 = 90^\circ$ is docked, the ligand becomes fully flexible in the quenching runs. The MC/SA protocol relaxes this structure, and Φ_3 never samples the region of space occupied by the sulfonamide in the crystal structure. While the absolute positioning of the sulfonamide is interesting, the main purpose of the docking procedure was to determine the position of the substituent on the 5-aryl ring. On the basis of FEP results presented below, it appears that the docking was successful in this regard.

The MC quenching runs were necessary in the docking process to distinguish between other alternative ligand conformations, although complexes resembling the crystal structure were often found during the first stage of docking. Figure 3 compares the structural results of two successive docking runs of **11** after (a) the Tabu stage of docking and (b) the MC quenching run. In each picture, the yellow structures correspond to the conformation of the ligand in the crystal structure, and the red and blue structures are conformations from different docking runs. The position of the protein was constant in both pictures and was removed for clarity. Note that both red structures are rotated by 180° around the aryl—aryl bisector, whereas the orientation of the blue structure more closely resembles the crystal structure conformation. After the Tabu search (Figure 3a), the complex containing the red structure is actually ca. 90 kcal/mol lower in energy than the corresponding blue complex. However, at the conclusion of the MC quenching

(41) Qiu, D.; Shenkin, P. S.; Hollinger, F. P.; Still, W. C. *J. Phys. Chem. A* **1997**, *101*, 3005–3014.

(42) Still, W. C.; Tempczyk, A.; Hawley, R. C.; Hendrickson, T. *J. Am. Chem. Soc.* **1990**, *112*, 6127–6129.

(43) Scarsi, M.; Apostolakis, J.; Caflich, A. *J. Phys. Chem. B* **1998**, *102*, 3637–3641.

(44) Jorgensen, W. L.; Chandrasekhar, J.; Madura, J. D. *J. Phys. Chem.* **1983**, *79*, 926–935.

(45) Jorgensen, W. L. *MCPRO*, Version 1.6; Yale University: New Haven, CT, 1999.

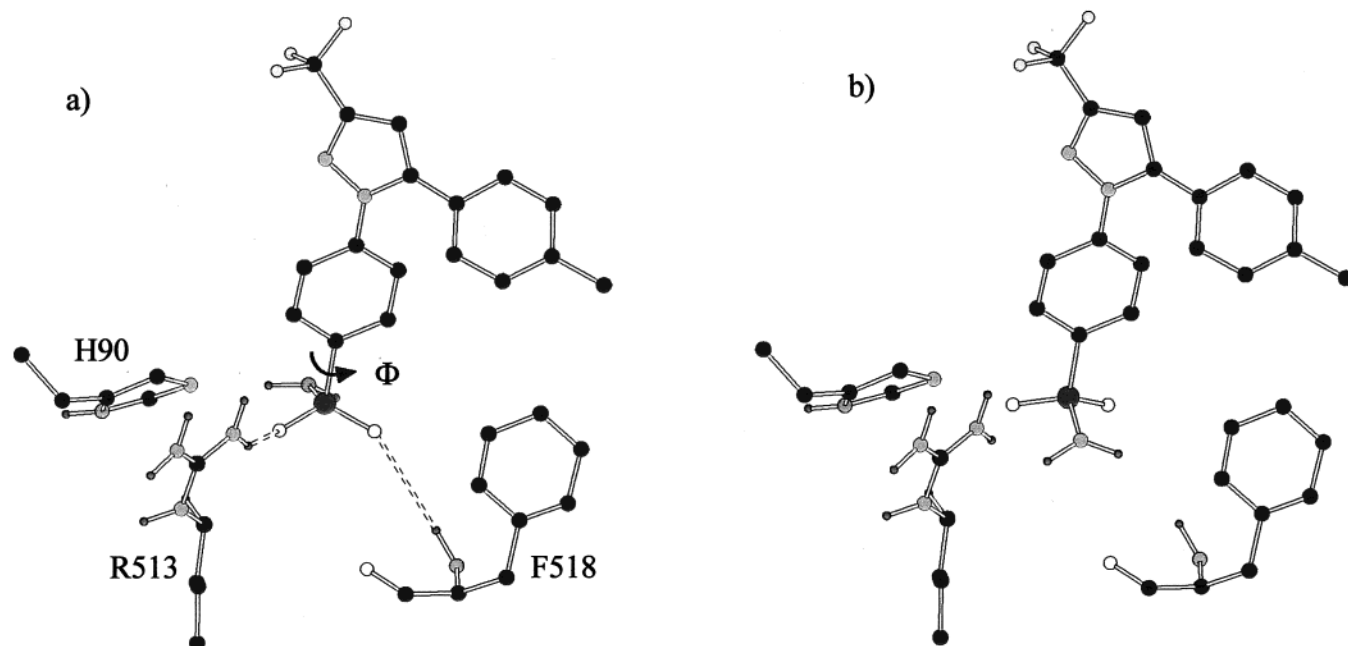


Figure 2. Ligand conformers used in docking with the sulfonamide dihedral equal to $+90^\circ$ (a) and -90° (b). Residues having hydrogen-bonding atoms within 3.2 Å of a sulfonamide oxygen atom are shown. In (a), both oxygen atoms make $O\cdots H-N$ interactions. In (b), no such interactions are formed. Hydrogens on carbon are not shown in many of the figures for clarity.

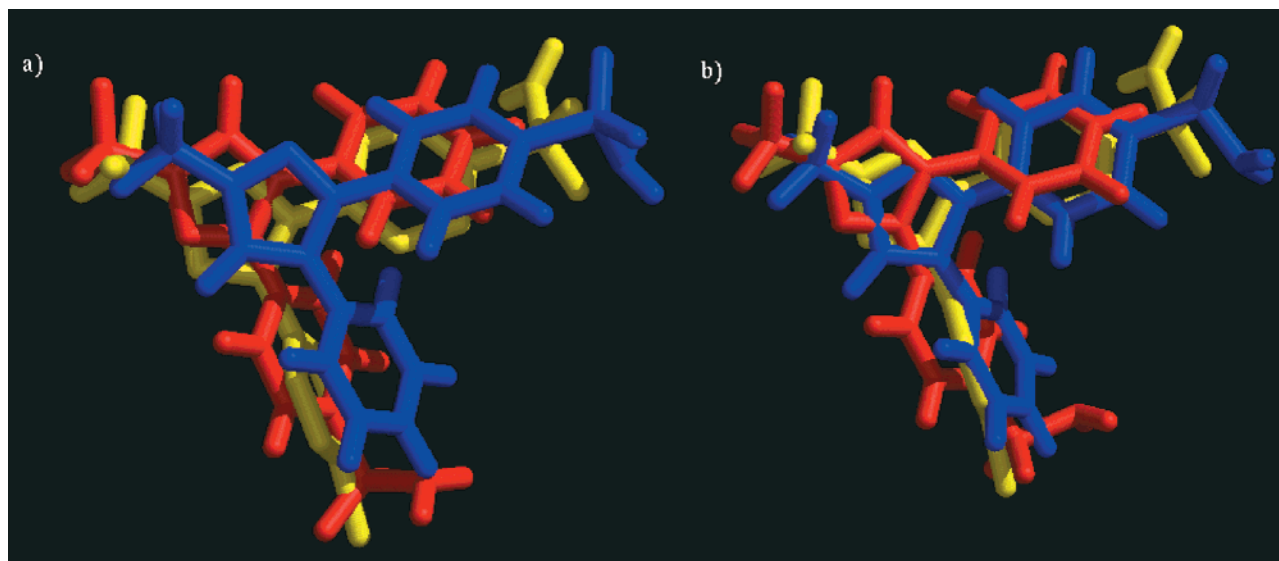


Figure 3. Binding conformations of **11** from the crystal structure (yellow) and from docking (blue, red). The protein has been removed for clarity. (a) Structures after the Tabu stage of docking. The complex containing the ligand conformation designated red in this picture is lower in energy than the corresponding blue complex. (b) Structures after both the Tabu and MC quenching stages. The blue complex is lower in energy than the red one. Molecular graphics images were produced using the MidasPlus system from the Computer Graphics Laboratory, University of California, San Francisco.⁴⁸

simulations (Figure 3b), the blue complex is ca. 10 kcal/mol lower in energy than the red one. In the absence of a crystal structure, one would have to rely on the results for the lowest-energy complex. In this case, the “correct” structure is lowest in energy only after both stages of docking have been completed. The final docked ligand was within 1.35 Å rmsd of the crystal structure, including the misplaced sulfonamide torsion.

FEP Results. Calculated relative binding free energies for the series of celecoxib derivatives are shown in Table 3. The results are in good agreement with the experimental data for binding to both isozymes.⁶ Free energy profiles for the representative transformations of **1** to **7** and **5** to **6** bound to COX-2 and from **3** to **4** in both COX enzymes are shown in Figure 4. In all cases, the free energy curves are smooth, and

the fluctuations are small. The hystereses for closing two binding cycles is small, as illustrated in Figure 5. Such hystereses are an important indicator of the statistical uncertainty in these calculations; hystereses of ca. 1 kcal/mol over four or five simulations are notably small.

Table 4 shows the free energy changes for binding to COX-2 relative to celecoxib **1** in order of decreasing affinity. The trend in calculated relative binding free energies agrees well with the experimental trend, as illustrated in Figure 6. The largest outlier is the hydrogen derivative **11**. This compound was predicted to be the most favorable binder, although the experimental data predict it to be less potent than **6**, **5**, and **9**, by at least 0.7 kcal/mol. The rationale for this discrepancy is discussed further below.

Table 3. Comparison of Experimental and Calculated Relative Binding Free Energies

A → B	exptl ^a		calcd		$\Delta\Delta G_{\text{binding}}$	
	ΔG_A	ΔG_B	ΔG_{aq}	ΔG_{COX}^b	exptl	calcd
3 → 4	-0.089	2.69	16.72 ± 0.12	19.28 ± 0.07	2.78	2.57
3 → 4	1.99	>4.09	16.72 ± 0.12	18.46 ± 0.10 ^c	2.10	1.74
3 → 5	-0.089	-2.79	15.80 ± 0.08	13.89 ± 0.09	-2.70	-1.91
3 → 6	1.99	0.56	15.66 ± 0.13	14.58 ± 0.11 ^c	-1.43	-1.08
3 → 1	-0.089	-1.91	19.92 ± 0.11	18.07 ± 0.17	-1.82	-1.86
3 → 1	1.99	1.60	19.92 ± 0.11	19.55 ± 0.17 ^c	-0.39	-0.37
5 → 6	-2.79	-2.86	2.12 ± 0.07	1.72 ± 0.09	-0.070	-0.40
6 → 8	-2.86	2.73	-14.28 ± 0.20	-7.75 ± 0.20	>5.59	6.53
1 → 7	-1.91	1.25	9.61 ± 0.06	12.73 ± 0.05	3.16	3.12
8 → 1	2.73	-1.91	17.75 ± 0.18	12.36 ± 0.11	<-4.64	-5.39
8 → 9	2.73	-2.73	17.40 ± 0.11	11.85 ± 0.03	<-5.46	-5.55
8 → 11	2.73	-2.04	19.28 ± 0.09	13.51 ± 0.06	<-4.77	-5.77
9 → 10	-2.73	-1.89	-1.90 ± 0.07	-1.94 ± 0.06	0.84	-0.04
10 → 11	-1.89	-2.04	2.31 ± 0.07	1.07 ± 0.11	-0.15	-1.24

^a Relative free energies are derived from the IC₅₀ values given in Table 1 using $\Delta\Delta G = \Delta G_2 - \Delta G_1 = RT \ln(K_1/K_2)$ using the approximation that the ratio of IC₅₀ values equals the ratio of dissociation constants.⁴⁷ ^b All data refer to binding to COX-2 unless otherwise noted. ^c Results for binding to COX-1.

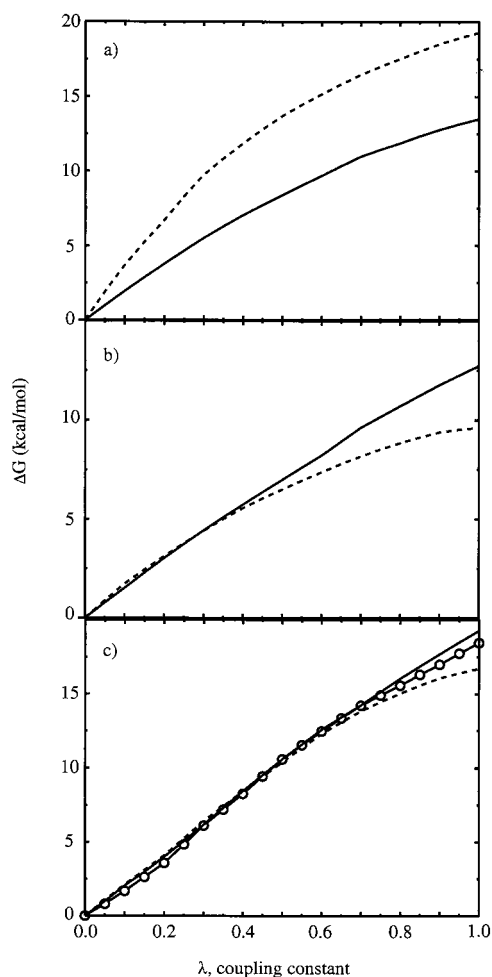


Figure 4. Free energy profiles for (a) 8 → 11, (b) 1 → 7, and (c) 3 → 4. The dotted lines represent data from the aqueous simulations, the solid lines illustrate free energy changes in COX-2 complexes, and the solid line with circles symbolizes COX-1 results.

In accord with structural data,^{14,20} the 5-aryl binding pocket is larger in COX-2 than COX-1, as evidenced in our simulations by the presence of a single water molecule bridging Ser⁵³⁰ and Tyr³⁸⁵ (Figure 7) in complexes with the former enzyme. This feature is not present in most of the COX-1 simulations, even though these two hydrogen-bonding residues are conserved in the two isozymes. While the possibility exists that the presence

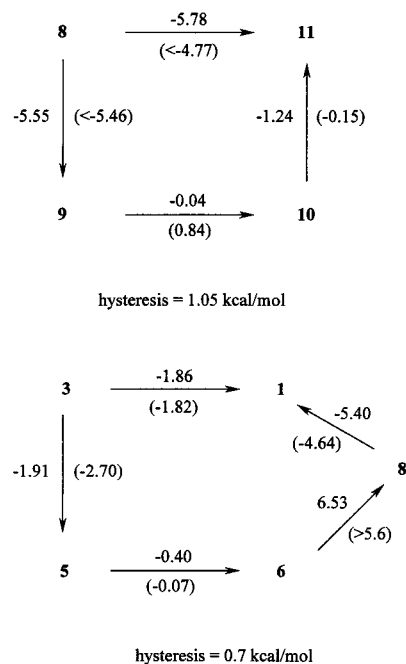


Figure 5. Calculated hystereses for closing perturbation cycles. Calculated and experimental (in parentheses) relative binding free energies in kilocalories per mole.

of the water molecule is an artifact of the procedure used to build the water cap in the simulations, it is not unlikely that this molecule binds in this position in view of the available hydrogen-bonding partners and the polarizability of the aromatic residues lining the cavity. Buried water molecules have been observed experimentally in much more hydrophobic cavities.⁴⁶

Steric Restrictions. Analysis of a space-filling representation of the binding site reveals that the binding pocket for the 5-aryl ring is long and narrow. The side of the binding site bordered by Tyr³⁸⁵ is quite sterically restricted. The opposite side is less congested. These observations are supported by the average binding positions from the MC/FEP simulations for ligands 3–6, as shown in Figure 8. In general, smaller substituents are

(46) Ernst, J. A.; Clubb, R. T.; Zhou, H.-X. *Science* **1995**, *267*, 1813–1817.

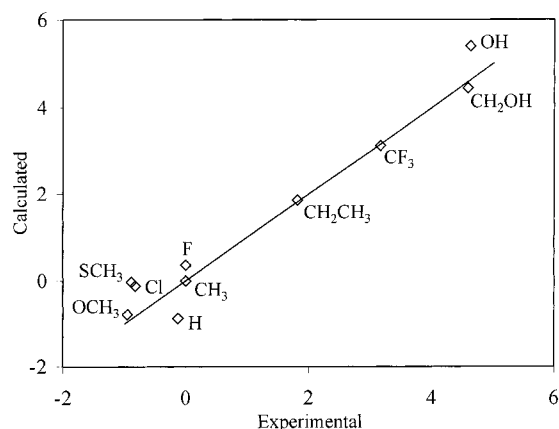
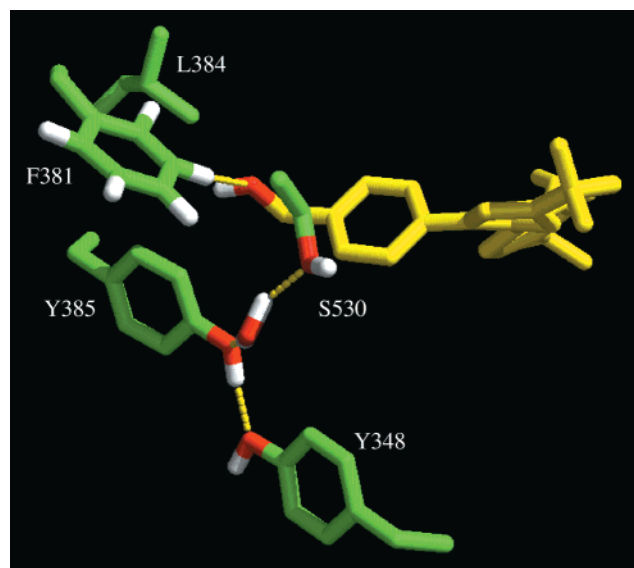
(47) Cheng, Y.; Prusoff, W. H. *Biochem. Pharmacol.* **1973**, *22*, 3099–3108.

(48) Ferrin, T. E.; Huang, C. C.; Jarvis, L. E.; Langridge, R. *J. Mol. Graphics* **1988**, *6*, 13–27.

Table 4. Experimental versus Calculated Binding Free Energies to COX-2 Relative to Celecoxib (1)

compound	calcd perturbation path ^a	$\Delta\Delta G_{\text{binding}}$ (kcal/mol)	
		calcd	exptl
6	$[-(8 \rightarrow 1) + -(6 \rightarrow 8)]; [-(3 \rightarrow 1) + (3 \rightarrow 5) + (5 \rightarrow 6)]^b$	-0.80 ± 0.31	-0.95
5	$-(3 \rightarrow 1) + (3 \rightarrow 5)$	-0.05 ± 0.24	-0.88
9	$-(8 \rightarrow 1) + (8 \rightarrow 9)$	-0.15 ± 0.24	-0.82
11	$[-(8 \rightarrow 1) + (8 \rightarrow 9) + (9 \rightarrow 10) + (10 \rightarrow 11)]; [-(8 \rightarrow 1) + (8 \rightarrow 1)]^b$	-0.90 ± 0.26	-0.13
1		0	0
10	$[-(8 \rightarrow 1) + (8 \rightarrow 9) + (9 \rightarrow 10)]; [-(8 \rightarrow 1) + (8 \rightarrow 11) + -(10 \rightarrow 11)]^b$	0.34 ± 0.26	0.01
3	$-(3 \rightarrow 1)$	1.86 ± 0.20	1.82
7	1 \rightarrow 7	3.12 ± 0.07	3.16
4	$-(3 \rightarrow 1) + (3 \rightarrow 4)$	4.43 ± 0.25	4.59
8	$-(8 \rightarrow 1)$	5.39 ± 0.21	4.63

^a See Table 3. ^b Computed $\Delta\Delta G_{\text{binding}}$ values are reported as averages of the two mutation pathways.

**Figure 6.** Calculated versus experimental free energies of binding for COX-2 ligands relative to celecoxib 1.**Figure 7.** Binding of ligand 4 to COX-2 from the Monte Carlo simulation. No hydrogen bond is formed between the ligand and the protein. The hydroxymethyl group interacts with Phe³⁸¹. One representative configuration of the complex is shown.

generally better binders. This trend is demonstrated in the perturbation of $3 \rightarrow 1$ by the fact that celecoxib 1 has a higher affinity than the ethyl derivative for COX-2 by ca. 1.8 kcal/mol.

Effect of H-Bond Donor ($3 \rightarrow 4$, $6 \rightarrow 8$, $8 \rightarrow 1$, $8 \rightarrow 9$, $8 \rightarrow 11$). In order for ligands 4 and 8 to bind to the receptor with high affinity, they must satisfy the hydrogen-bonding capability of the hydroxyl or hydroxymethyl substituent. This type of interaction with the receptor can occur only with Tyr³⁸⁵,

as Ser⁵³⁰ is too far away. However, the hydroxyl substituents are forced to point away from Tyr³⁸⁵ to accommodate the steric restrictions noted above (Figure 7).

There is an additional steric issue involved in the low binding affinity of ligand 4. As mentioned above, the side of the binding site occupied by Tyr³⁸⁵ is sterically hindered. In addition, the sulfur of Met⁵²², on the opposite side of the binding site, lies at the surface of the cavity. Therefore, neither side is a favorable location for the oxygen atom of the hydroxymethyl group. Consequently, the substituent adopts an extended conformation that minimizes unfavorable interactions. In the gas phase, this orientation for the hydroxymethyl group is 1.9 kcal/mol higher in energy than an alternative conformation (Figure 9). The aryl CH \cdots O interaction at ca. 2.5 Å between the hydroxyl oxygen atom of the ligand and Phe³⁸¹ (Figure 7) may help stabilize this conformation when the ligand is bound to the receptor.

Effect of an Electron-Withdrawing Group ($1 \rightarrow 7$). The calculated relative binding free energy (Table 3) for the mutation of the methyl to trifluoromethyl substituent is 3.15 ± 0.08 kcal/mol. This value is in good agreement with the experimental data (3.16 kcal/mol). The transformation from $1 \rightarrow 7$ in the gas phase yields a free energy change of 6.85 ± 0.01 kcal/mol. When combined with the change in free energy in solution (9.61 ± 0.06 kcal/mol), the hydration free energy difference is 2.76 kcal/mol, in favor of the methyl compound. Therefore, in order for the trifluoromethyl compound to be a poorer binder, there must be a 6 kcal/mol free energy preference for 1 in the complex.

One would expect that the electron-withdrawing character of the trifluoromethyl group may reduce favorable interactions between the 5-aryl ring and aromatic residues Phe³⁸¹, Tyr³⁸⁵, Trp³⁸⁷, and Phe⁵¹³ lining the binding site (Figure 10). In an effort to quantify such interactions in the gas phase, several conformers of complexes of benzene with either toluene or trifluoromethylbenzene were examined. Calculated differences in interaction energies between the toluene complexes and the corresponding trifluoromethylbenzene complexes did not clearly support this hypothesis. Thus, unfavorable van der Waals contacts for the larger trifluoromethyl group at the top of the binding site (Figure 1) are likely the dominant factor for the reduced binding affinity.

Advantage of Using Docking To Predict Starting Conformations. The importance of performing the docking protocol in order to obtain starting positions for the FEP simulations was confirmed by calculations that were started from nonoptimal conformations. For example, in the case of the perturbation of $5 \rightarrow 6$, a difference of over 1 kcal/mol was obtained for the bound ΔG , depending on the starting conformation of 5. There are two orientations that place the thiomethyl group at the preferred gas-phase position of $\pm 90^\circ$. Two separate bound

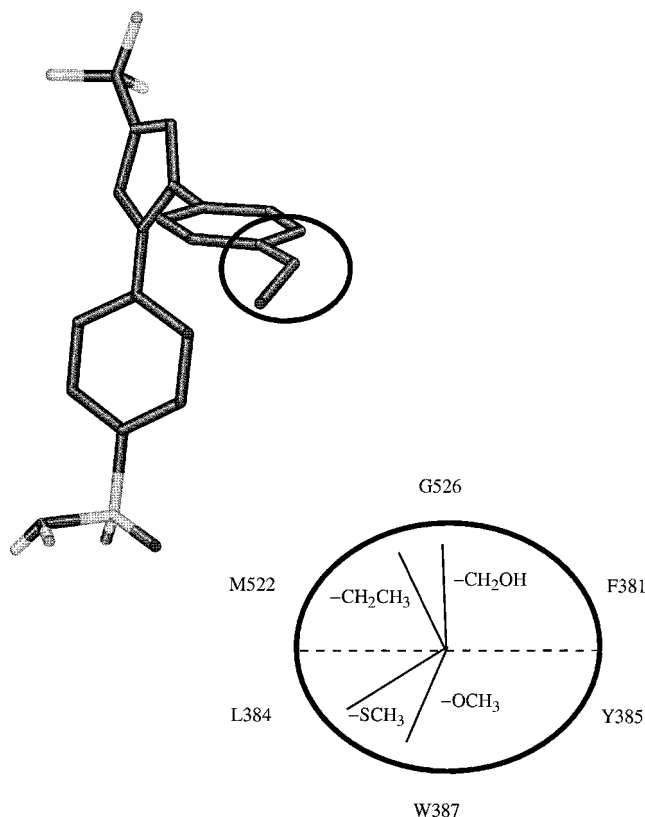


Figure 8. Average binding conformations for ligands 3–6. The ellipse symbolizes a cross-sectional region of space in the binding site.

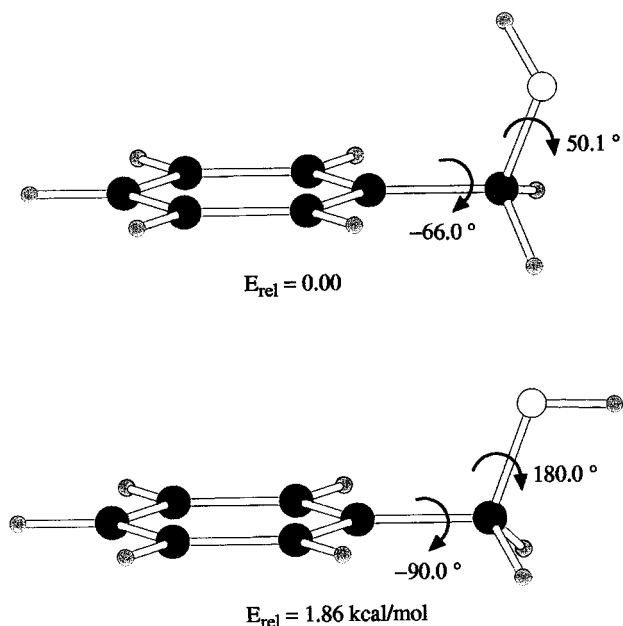


Figure 9. Gas-phase conformational energies of benzyl alcohol as a model compound for ligand 4.

simulations were run, beginning with the C–C–S–C dihedral equal to $+90^\circ$ and -90° . The calculated changes in free energy for the two simulations were 0.60 ± 0.08 and 1.72 ± 0.09 kcal/mol. When combined with the calculated free energy change for this perturbation of the ligand in solution (2.12 ± 0.07 kcal/mol), the relative binding free energies are -1.52 ± 0.11 and -0.40 ± 0.11 kcal/mol, respectively. The former calculation predicts the methoxy analogue to be a significantly better binder than the thiomethyl derivative. However, according to the latter calculation and the experimental data (Table 1), they bind

equally well. The energy barriers are apparently large enough to prevent movement of the thiomethyl substituent from one face of the ring to the other during the simulations. The conformer that yielded a relative binding free energy in agreement with experiment was, indeed, the one which was predicted by the docking studies to bind more favorably. The same pattern was observed for simulations involving the ethyl derivative **3**. Therefore, the docking studies were able to determine which of these conformers should be used as the starting point for the FEP simulations. In the absence of the docking calculations, the need for multiple FEP calculations with different starting conformations is apparent.

Anomalous Results for Unsubstituted Derivative 11. As mentioned above, the MC/FEP simulations predict the relative binding free energy of unsubstituted ligand **11** to be too favorable, as shown in Table 4. Analysis of the binding site during the mutation of **10** to **11** reveals that an additional water molecule is positioned in the cavity. This water molecule makes two hydrogen bonds to Met⁵²², one to the backbone carbonyl, and another to the sulfur atom (Figure 11). In addition, the oxygen of the water molecule is positioned for interaction with the 4-substituent on the 5-aryl ring. The charge on the fluorine atom in ligand **10** is -0.09 , compared to $+0.17$ on the hydrogen in **11**. Therefore, the electrostatic interaction at this site with the negatively charged oxygen atom of the water molecule is favorable for ligand **11** and repulsive for ligand **10**, which can account for the calculated preferred binding of the former.

It is unclear whether this water molecule should actually be present in the cavity with the smaller ligands. To determine the effect of the bridging water molecule, the water molecule was manually removed from the binding site, and the simulation **10** \rightarrow **11** was rerun. The free energy change for this new simulation of the complex was 3.83 kcal/mol. When combined with the corresponding free energy change in solution (Table 3), the relative free energy of binding is 1.52 kcal/mol. Thus, in the absence of the bridging water molecule, the unsubstituted compound binds more poorly than the fluoro compound. The possibility that there is partial occupancy by a water molecule is a challenge beyond the sampling capabilities of the present simulations.

It is also possible that the protein undergoes a conformational change in the presence of the smaller ligands (i.e., **9–11**). In fact, a (COX-1)Phe \rightarrow (COX-2)Leu substitution at position 503 is thought to increase the flexibility of COX-2 in this region of the binding site.³ However, our simulations do not include backbone flexibility after the initial conjugate gradient minimization, and therefore subsequent conformational changes in the backbone are not included.

The presence of the water molecule in the cavity introduces intermolecular electrostatic interactions that overestimate the binding affinity of the unsubstituted compound. On the other hand, the absence of the water molecule creates a void in the binding site which results in underestimation of the free energy of binding for this ligand. The two scenarios cause the computations to bracket the “correct” binding free energy.

Positioning of the Sulfonamide and COX-2/COX-1 Selectivity. As mentioned above, the docking runs predicted that the sulfonamide group binds in a different conformation than suggested by the 1cx2 crystal structure. To quantify the energetic preference, an FEP transformation was performed on ligand **6** bound to COX-2 between the crystal structure position and the docked position of the sulfonamide (Figure 12). This mutation

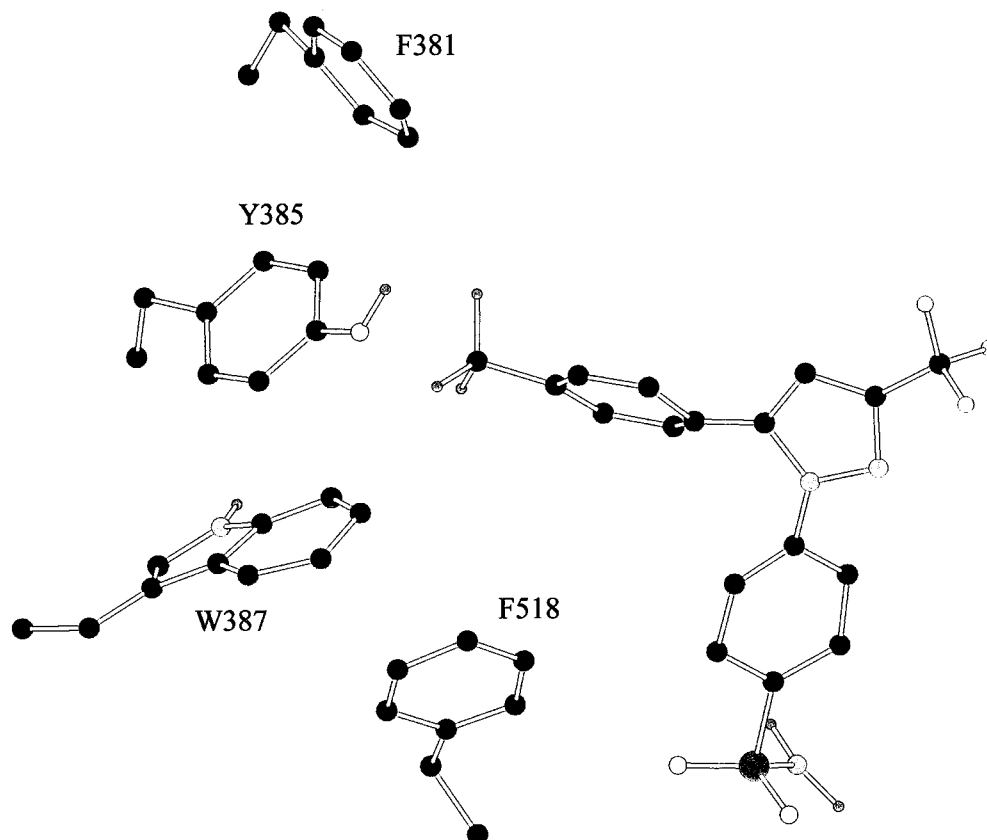


Figure 10. Potential aromatic–aromatic interactions in the binding site.

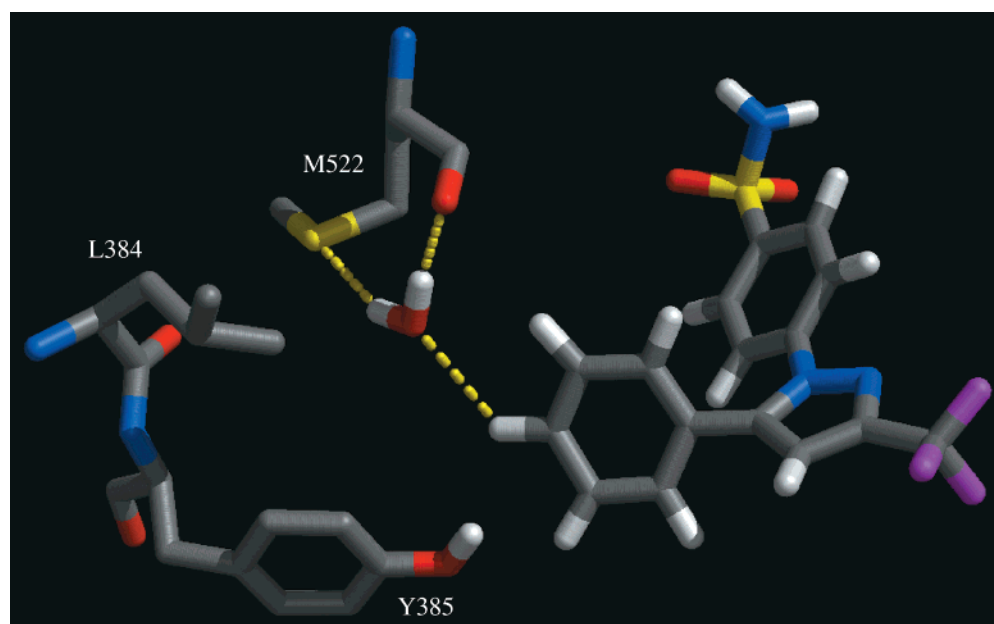


Figure 11. A water molecule in the binding site bridges the ligand and receptor. One representative configuration from the Monte Carlo simulation is shown.

involved “shrinking” the two hydrogen atoms on the sulfonamide to dummy atoms and converting the nitrogen atom to an oxygen atom while simultaneously converting one of the sulfonamide oxygen atoms to a nitrogen atom and “growing” out its hydrogen atoms. This protocol was used in lieu of simply driving the dihedral angle of the sulfonamide because larger fluctuations in the free energy changes could be expected using the latter procedure.

The position of the sulfonamide predicted in the docking studies was preferred over the crystal structure orientation by

4.53 ± 0.16 kcal/mol. This strong preference seems to arise from several factors. First, in the 1cx2 structure position, one of the oxygen atoms makes unfavorable electrostatic interactions with the amide carbonyl oxygen of Gln¹⁹² and the backbone carbonyl oxygen of Ser³⁵³ (Figure 12a). In addition, one of the amide hydrogen atoms does not form a hydrogen bond. However, in the new conformation, the NH–O hydrogen bonds are formed with Gln¹⁹² and Ser³⁵³, and the hydrogen bond donated by a water molecule to the sulfonamide N is maintained. There is also favorable electrostatic interaction with Arg⁵¹³,

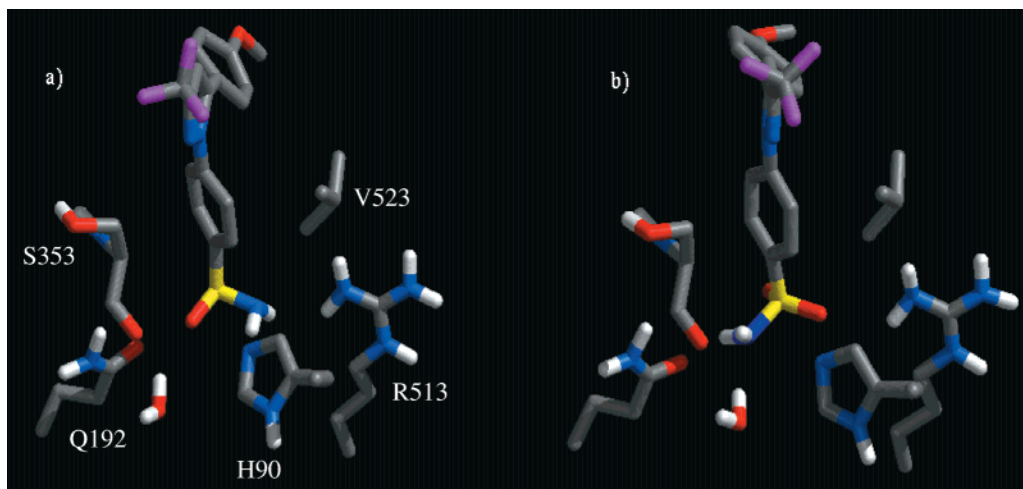


Figure 12. Initial (a) and final (b) structures from the perturbation of the sulfonamide conformation, corresponding to conformers presented in 1cx2 and 6cox crystal structures, respectively.

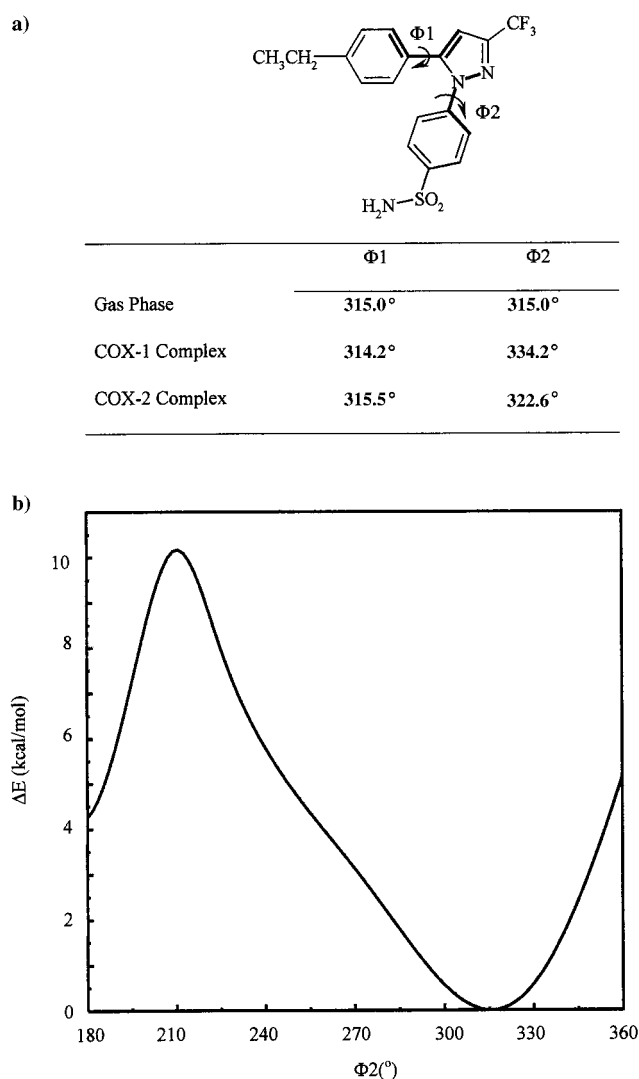


Figure 13. Proposed effect of the COX-1 Ile⁵²³ → COX-2 Val⁵²³ substitution. (a) Dihedral angles from the complexes are average values over 5 million configurations of an MC/FEP simulation. (b) Optimized relative energies as a function of $\Phi 2$ angle. $\Phi 1$ was fixed at -315° during these optimizations.

though it is beyond the hydrogen-bonding range. In addition, this preference would most likely be even greater when His⁹⁰ is in the other tautomeric form or is protonated because the

hydrogen bond to the amino group in the crystal structure would be lost, and one to the sulfonamide oxygen in the predicted conformation would be gained. The following question arises from this result: if the single amino acid substitution of Ile in COX-1 for Val in COX-2 at position 523 is sufficient to confer COX-2 selectivity of these ligands,¹⁸ and the amino group does not extend into the pocket created by the smaller valine residue, how does this residue affect selectivity? Visual analysis of the complex suggests that that additional methyl group of Ile⁵²³ compared to valine may lead to unfavorable contacts with the proximal sulfonamide oxygen and the adjacent benzene ring.

To seek evidence for such potential strain, average values for dihedral angles of the two torsions governing the positions of the benzene rings from the MC/FEP simulations were compared to gas-phase dihedral preferences for compound **3**. As shown in Figure 13a, the position of $\Phi 1$ remains close to the value of the angle in the gas phase. However, $\Phi 2$ deviates from the preferred gas-phase value in both COX-1 and COX-2, although a larger difference is seen when the ring is bound to the former isozyme. To determine the changes in internal energy between the different positions of these rings, a series of gas-phase optimizations for the ligand was performed where $\Phi 1$ was held fixed at -315° and $\Phi 2$ was varied between 180° and 360° . A plot of the resulting relative energies (Figure 13b) as a function of $\Phi 2$ indicates that there is a ca. 0.3 kcal/mol difference between the gas-phase position and the conformation found in COX-2. However, the conformation in COX-1 is destabilized by over 1 kcal/mol relative to the gas phase. In addition to this internal energy difference, the altered position of the 5-aryl ring when bound to COX-1 may also adversely affect the aromatic–aromatic interactions with Phe⁵¹⁸ and the van der Waals interaction with the backbone of Ser³⁵³.

Thus, the results support the hypothesis that the Val-to-Ile substitution leads to adverse steric effects, which are reflected in the altered conformation and positioning of the benzene ring. Further analysis would be aided by an FEP study of the Val-to-Ile mutation to verify that the simulations quantitatively reflect the observed COX-2/COX-1 selectivity.

Conclusion

This work illustrated the value of a novel docking procedure for determining starting conformations for FEP calculations, the quantitative accuracy that can then be obtained with current MC/FEP methodology, and the accompanying structural and ener-

getic insights that can be obtained into the features governing protein–ligand binding.

While improved sampling of internal degrees of freedom in the ligand seems necessary for ideal docking results, the present predetermination of favored conformations provided viable starting positions for the FEP simulations. In general, use of the conformer library was valuable for identifying alternative binding conformations, e.g., for the sulfonamide and thiomethyl substituents. Finally, the docking results provided the motivation to examine the sulfonamide conformation, and thus the COX-2/COX-1 selectivity, in greater detail.

The MC/FEP simulations yielded relative binding free energies in excellent agreement with the experimental data for all compounds tested, and the structural results help explain several experimentally observed trends. First, steric hindrance restricts access of the ligand's substituents to some regions of the binding pocket and thus affects binding affinity. In addition, ligands that contain hydrogen-bonding functionality at the 4-position of the 5-aryl ring are poor binders because hydrogen bonds cannot be formed between the substituents and the surrounding protein residues.

Further analysis of the binding orientation of the sulfonamide indicated that this substituent adopts the conformation presented in the crystal structure 6cox. The experimental selectivity arising from the Val → Ile substitution at position 523 in COX-1 compared to COX-2 can be explained by adverse steric effects, which are reflected in the altered orientation of the phenylsulfonamide ring.

Overall, the combined docking and Monte Carlo methodology accurately models a variety of effects including internal energy differences, solvation, sterics, and intermolecular interactions. In particular, the ease with which these MC/FEP simulations can be performed due to the quantum-mechanical determination of charges and docking prediction of binding conformations makes this combined protocol useful for lead optimization in a drug design scenario.

Acknowledgment. Gratitude is expressed to Dr. Willem P. van Hoorn for his contributions to MATADOR and to the National Institutes of Health (GM32136) for financial support.

JA001018C